Acta Oceanol. Sin., 2019, Vol. 38, No. 4, P. 116–125
https://doi.org/10.1007/s13131-019-1417-3
http://www.hyxb.org.cn
E-mail: hyxbe@263.net

The interactions between surface Kuroshio transport and the eddy field east of Taiwan using satellite altimeter data

Huizan Wang[1, 2*], Quanhong Liu[2], Hengqian Yan[2], Bo Song[2], Weimin Zhang[2]

[1] State Key Laboratory of Satellite Ocean Environment Dynamics (SOED), Second Institute of Oceanography, Ministry of Natural Resources, Hangzhou 310012, China

[2] College of Meteorology and Oceanography, National University of Defense Technology, Changsha 410073, China

Received 8 February 2018; accepted 19 June 2018

Abstract

Based on the daily sea surface height and absolute geostrophic velocity data from 1993 to 2015 provided by the AVISO Center of French Space Agency, the surface Kuroshio transport east of Taiwan and its adjacent eddy field (sea surface height anomaly) were analyzed. Four main periods of the surface Kuroshio transport and eddy field east of Taiwan were obtained, which were used to reveal their interactions. The main conclusions are as follows: (1) Based on the wavelet analysis, the surface Kuroshio transport east of Taiwan and its nearby eddy field showed significant seasonal, annual and interannual periods. In addition to the obvious periods of 182 days (0.5 year) and 365 days (1 year), there were also more obvious periods of about 860 days (2.35 years) and 2 472 days (6.8 years) for the surface Kuroshio transport. There were also four more obvious periods corresponding to the eddy field of 200 days (0.55 year), 374 days (1 year), 889 days (2.43 years) and 2 374 days (6.5 years), although there were latitudinal variations. (2) Based on both the correlation and causal analysis, the correlation between the surface Kuroshio transport and the nearby eddy field over the above four periods was analyzed, and different Kuroshio-eddy interactions, with period and latitudinal variability, were revealed.

Key words: wavelet analysis, causal analysis, Kuroshio east of Taiwan, correlation, sea level anomaly

Citation: Wang Huizan, Liu Quanhong, Yan Hengqian, Song Bo, Zhang Weimin. 2019. The interactions between surface Kuroshio transport and the eddy field east of Taiwan using satellite altimeter data. Acta Oceanologica Sinica, 38(4): 116–125, doi: 10.1007/s13131-019-1417-3

1 Introduction

As one of the major western boundary currents, the Kuroshio carries momentum and heat northward from the tropics to mid-latitude regions. It plays a vital role in ocean circulation and affects climate and fisheries across the coastal regions of northeast Asia. The Kuroshio east of Taiwan shows tremendous variability (Jan et al., 2015), with an overall mean transport of 21.5 Sv (1 Sv=10^6 m^3/s) (Johns et al., 2001).

Mesoscale eddies are nearly ubiquitous in the world's ocean (Wang et al., 2003; Chelton et al., 2011; Nan et al., 2011a; Zheng et al., 2017), especially in the region over the subtropical countercurrent (STCC) (Hwang et al., 2004; Qiu and Chen, 2010a). Eddy trajectory statistics have indicated that eddies frequently intrude into the Kuroshio regime at two latitude bands, at the Luzon Strait and east of Taiwan (Lee et al., 2013; Cheng et al., 2017). Ma et al. (2016) showed that the feedback between ocean mesoscale eddies and the atmosphere is fundamental to the dynamics and control of the Kuroshio, highlighting the importance of eddies for the Kuroshio. When the westward-propagating mesoscale eddies, with an average propagation velocity of about 9 cm/s, encounter the east of Taiwan, they will interact with the Kuroshio, influencing its current and path (Hwang et al., 2004).

Satellite and *in situ* observations (Yang et al., 1999; Hwang et al., 2004; Qiu and Chen, 2010b) and simulated results (Geng et al., 2016, 2018; Kuo et al., 2017) have indicated the existence of eddy-Kuroshio interactions. Interpretations have included the effects of the Kuroshio on eddies, which appear to decay near the western boundary, and how eddies drive Kuroshio variability (Chang and Oey, 2011; Nan et al., 2011b; Ma and Wang, 2014; Lien et al., 2014; Tsai et al., 2015; Chang et al., 2015; Delman et al., 2015). Kuroshio variations in the East China Sea (ECS) are induced by mesoscale eddies east of Taiwan (Ichikawa et al., 2008; Hsin et al., 2011), and eddies with a radii larger than 150 km are strong enough to significantly alter the Kuroshio (Zheng et al., 2011). The impact of eddies on the Kuroshio volume transport has long been recognized: eddies from the STCC play an important role in affecting Kuroshio transports both at interannual and seasonal time scales (Qiu and Chen, 2010a), and approaching anticyclonic (cyclonic) eddies result in an increase (reduction) of the Kuroshio transport (Yang et al., 1999; Zhang et al., 2001; Lee et al., 2013). The westward propagating eddy can also trigger the Kuroshio to meander or intrude (Waseda et al., 2002; Miyazawa et al., 2004; Hsu et al., 2016; Yin et al., 2017). Anticyclones can also intensify sea surface and pycnocline slopes across the Kuroshio, while cyclones weaken these slopes, particularly east of Taiwan (Tsai et al., 2015). Furthermore, mesoscale eddies can be shed from the Kuroshio loop (Zhang et al., 2017; Liu et al., 2017).

Most of these described results led to the conclusion that an-

Foundation item: The National Key R&D Program of China under contract No. 2018YFC1406202; the National Natural Science Foundation of China under contract Nos 41206002, 41706021, 41775053 and 91428206; the China Postdoctoral Science Foundation under contract No. 2014M551711.

*Corresponding author, E-mail: wanghuizan@126.com

ticyclonic eddies correspond to an increase in transport and cyclonic eddies are related to transport reduction. However, contrasting results have also been reported (Zhang et al., 2001). Yan et al. (2016) found that both anticyclonic and cyclonic eddies can strengthen or weaken the Kuroshio volume transport. The relationship between the mesoscale eddy field and the Kuroshio is more complicated and even partially contradictory because of the scarcity of ocean observational data and nonlinear phenomena (Zheng et al., 2011).

Previous research on Kuroshio and eddy variability have often regarded the Kuroshio and the eddies east of Taiwan as a whole and focused less on their different characteristics at different latitudes. Concurrently, to a certain extent, the observations have been limited in time resolution, generally more than 7 days, and the length of time series, generally less than 10 years. Most of the studies have been model-based, and it is unclear if their results are fully applicable to real eddy-Kuroshio interaction (Geng et al., 2016).

Although many works have shed light on the variations of mesoscale eddies or the Kuroshio east of Taiwan, few studies have discussed the interaction between the eddy field and Kuroshio over different time scales, especially the effect of the Kuroshio on the nearby eddy field. In addition, a longer record measurement period will be needed to resolve the variations in the Kuroshio and eddies. Different Kuroshio-eddy interactions over varying time periods and latitudes remains to be quantified and further studied.

The objective of this paper is to characterize the variability in the Kuroshio and eddy field (sea level anomalies) east of Taiwan, understand the correlation between the sea level anomaly filed (westward-propagating mesoscale eddies) and the Kuroshio, and to unravel the cause-effect relation between them .

This paper is organized as follows: Section 2 describes the data source and methodology. Section 3 analyzes the periods of the surface Kuroshio and nearby eddy field. In Section 4, the correlation and cause-effect relation between the sea level anomaly field (westward-propagating mesoscale eddies) and the Kuroshio are revealed. The results are summarized in Section 5.

2 Data source and methodology

2.1 *Satellite altimeter data*

The satellite-derived daily sea level anomaly (SLA) data and surface current data (MADT_UV) (a total of 8 400 d) with delayed quality control were provided by the AVISO (Archiving, Validation, and Interpretation of Satellite Oceanographic) data center, the data was merged from multi-satellite altimeter data of T/P, Jason-1/2 and Geosat and other orbiting satellites. The product was gridded to 0.25°×0.25° and a time interval of 1 d. The time ranges from January 1993 to December 2015, a total of 23 years with 8 400 d. The study area is east of Taiwan (22.5°–25°N, 121°–125°E).

2.2 *Surface Kuroshio intensity (SKI)*

Surface current data is also provided by AVISO center to identify the Kuroshio axis and compute the surface Kuroshio intensity (SKI).

As a strong western boundary current, the most prominent feature of the Kuroshio is its velocity. The Kuroshio axis is defined as the line of the maximum surface velocity along the Kuroshio path.

Using the surface geostrophic velocity, the SKI (INT_{v_g}) can be calculated from

$$INT_{v_g}=\int_{X_W}^{X_E} v_g(x,y,t)\mathrm{d}x, \tag{1}$$

where x, y and t are longitude, latitude and time, respectively; X_W and X_E are the western and eastern integral limits; and v_g is the surface current from AVISO (MADT_UV). X_W follows the eastern coastline of Taiwan; however, the eastern integral limit, X_E, is set to the position of Kuroshio axis +1 (plus one longitude) (Hsin et al., 2013; Wang et al., 2018).

The identification of the Kuroshio axis was based on the surface currents by Ambe et al. (2004). Wang et al. (2018) identified the daily axis of the Kuroshio east of Taiwan and investigated the variation in axes position and SKI for different latitudes based on the 23-year (1993–2015) satellite-derived daily surface current data. The daily SKI dataset is based on the method of Wang et al. (2018).

2.3 *Selection of related eddy field*

To obtain the continuous time series of the mesoscale eddies approaching the Kuroshio east of Taiwan, the regional sea level anomaly field (22.5°–25°N, 123°–124°E) was used to characterize the mesoscale eddies (Fig. 1). The region selected for the eddy field was a compromise between the areas approaching the Kuroshio region and mixing with the Kuroshio. The advantage of the SLA field is that it is continuous compared to the mesoscale eddies. In this study, the time series of the mean SLA averaged from 123°E to 124°E was used as the time series of eddy field for each latitude.

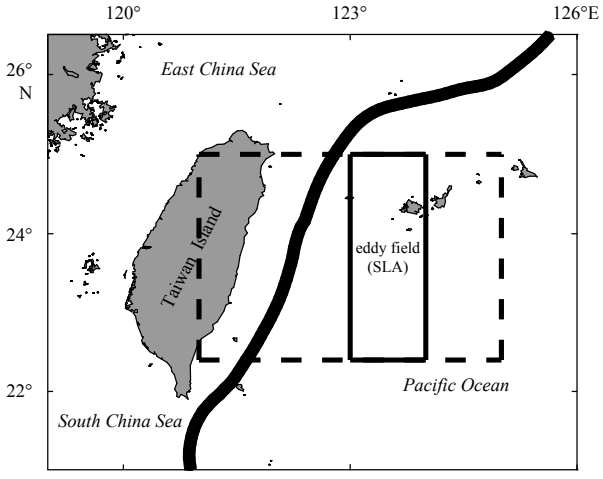

Fig. 1. Study area. The outer dotted box represents the study area of the Kuroshio and the inner solid box the research area of the eddy.

2.4 *Wavelet analysis*

Wavelet analysis is a widely-used method to analyze localized variations of power within a time series (Torrence and Compo, 1998; Yu et al., 2007). By decomposing a time series into the time–frequency space, both the dominant modes of variability and how those modes vary over time can be determined. For a detailed introduction to wavelet analysis, please refer to Torrence and Compo (1998).

In this study, wavelet analysis was used to calculate the wavelet power spectra at different latitudes respectively for the time

series of the SKI and mean sea level anomalies. By calculating the power spectra at different latitudes, four corresponding obvious seasonal and interannual periods were identified.

2.5 *Correlation analysis*

Previous studies have showed a good correlation between the Kuroshio volume transport east of Taiwan and the sea surface height (Yang et al., 2014), and found a maximum correlation of 0.83 between PCM-1 Kuroshio transport and sea surface height anomalies at 23.9°N, 123.2°E (Gawarkiewicz et al., 2011).

To understand the correlation between the sea level anomaly field (westward-propagating mesoscale eddies) and SKI, we first calculated the correlation coefficient between the two variables. Except for the correlation between the surface Kuroshio intensity and the eddy at the same time, the time-lagged correlation between the surface Kuroshio intensity and the eddy fields for different lag times were also calculated. Using these calculations, we obtained the correlation coefficients for surface Kuroshio intensity and eddy across a range of latitudes for different lag times and periods.

After computing the correlation coefficients, the significance of the correlation coefficient should be tested. The statistic obeys the t distribution with a degree of freedom of n–2. The correlation coefficient is derived from the formula for the critical value:

$$r_\alpha = \frac{t_\alpha}{\sqrt{{t_\alpha}^2 + (n-2)}}. \tag{2}$$

Based on the significant level of $\alpha = 0.05$, degree of freedom of n=8 400, and checking t distribution threshold table to obtain $t_\alpha = 1.96$, we determined that the correlation coefficient passed the test if $r_\alpha > 0.021\ 4$ based on Eq. (2).

2.6 *Causal analysis*

Recently, a rigorous yet concise formula has been derived to evaluate information flow, and hence the causality in a quantitative sense, between time series (Liang, 2014). To assess the importance of a resulting causality, the time series need to be normalized. The normalization is achieved by distinguishing a Lyapunov exponent-like, one-dimensional phase-space stretching rate, and noise-to-signal ratio from the rate of information flow in the balance of the marginal entropy evolution of the flow recipient (Liang, 2015).

Using the method provided in Liang (2015), take two series X_1 and X_2, for example. C_{ij} is the sample covariance between X_i and X_j, and $C_{i,\mathrm{d}j}$ is that between X_i and $\dot{X}_j$, $\dot{X}_j$ being the difference approximation of $\mathrm{d}X_j/\mathrm{d}t$ using the Euler forward scheme (Liang, 2014). In addition, $\frac{\mathrm{d}H_1}{\mathrm{d}t}$ is the rate of change of the marginal entropy of X_1. It can be decomposed into two parts, $\frac{\mathrm{d}H_1^*}{\mathrm{d}t}$ and $\frac{\mathrm{d}H_1^{\mathrm{noise}}}{\mathrm{d}t}$.

Through the following equations:

$$T_{2\to1} = \frac{C_{11}C_{12}C_{2,d1} - C_{12}^2 C_{1,d1}}{C_{11}^2 C_{22} - C_{11}C_{12}^2}, \tag{3}$$

$$Z_{2\to1} \equiv |T_{2\to1}| + |\frac{\mathrm{d}H_1^*}{\mathrm{d}t}| + |\frac{\mathrm{d}H_1^{\mathrm{noise}}}{\mathrm{d}t}|, \tag{4}$$

$$\tau_{2\to1} = T_{2\to1}/Z_{2\to1}, \tag{5}$$

we have drawn the causal relationship between the surface Kuroshio intensity and the eddy field. The method provided in Liang (2015) provided a mechanism for normalizing the results so that the interaction between the two were directly compared using $\tau_{2\to1}$ and $\tau_{1\to2}$.

This study adopted the method provided by Liang (2015) to evaluate the causal relationship between time series of the sea level anomaly filed (westward-propagating mesoscale eddies) and the SKI. Furthermore, we were able to reveal these causal relationships between the surface Kuroshio intensity and eddy field at different latitudes over different periods.

3 Variation of surface Kuroshio intensity and eddy field

3.1 *Variation of surface Kuroshio intensity*

The time series of surface Kuroshio intensity from January 1993 to December 2015 are analyzed by wavelet analysis described above, and its wavelet power spectrums for different latitudes are obtained. Taking the Kuroshio at latitudes of 23°N and 25°N as examples, the corresponding wavelet power spectra are provided in Figs 2 and 3. Color indicates the significance of the period, with colors closer to red indicating more pronounced periodicity. The thin black line is the cone of influence (COI), and the power spectrum outside the curve is not considered due to the boundary effect (Yu et al., 2007). From these figures, there are clear seasonal and interannual variations in the SKI. When the wavelet analysis method is used to identify a periodic wave in a time series, in addition to passing a significance test, the periodic wave time series must be within a COI.

Based on the average power spectrum at different latitudes from 22.5°N to 25°N, e.g., in Figs 2c and 3c, the power spectra of the SKI time series at all latitudes were obtained. In Fig. 4, periods of 182 days (0.5 year, the semiannual period), 365 days (1 year, the annual period), 860 days (2.35 years, the first interannual period), 2 472 days (6.8 years, the second interannual period) are obvious. Furthermore, different periods occur at different latitudes in the SKI time series. The periodicity of the semiannual period and 2.35-year periods at the lower latitudes (22.5°–24°N) is more pronounced than that in the higher latitudes (24°–25°N) east of Taiwan. The annual period and 6.8-year period in each latitude have good periodicity and the 6.8-year period at the lower latitudes (22.7°–23.9°N) is most significant. It should be noted that many previous studies (Zhang et al., 2001) have shown a 100-day variability in the Kuroshio based on the PCM1 data at about 24.5°N, which is also observed in Fig. 3 (the period is 115 days accurately). However, the 100-day period is not as significant as other periods, such as the semiannual or annual cycle.

Once these data were obtained, a significance test was performed, and the power spectrum is shown in Fig. 5a. The blank areas are the regions that failed the test, where the results do not meet the significance threshold. The remaining regions passed the test, and are considered significant.

3.2 *Variation of eddy field*

The power spectra for the time series of the eddy fields to the east of the Kuroshio (sea level anomalies) at different latitudes were also obtained based on wavelet analysis. The corresponding wavelet power spectra of eddy fields at latitudes of 23°N and 25°N were obtained (Figs 6 and 7). As shown in these figures, there are seasonal and interannual variations in the eddy fields east of Taiwan.

Based on the average power spectra at different latitudes from 22.5°N to 25°N, e.g., Figs 6c and 7c, the time series power spectra for eddy fields at all latitudes east of Taiwan were obtained (Fig. 5b).

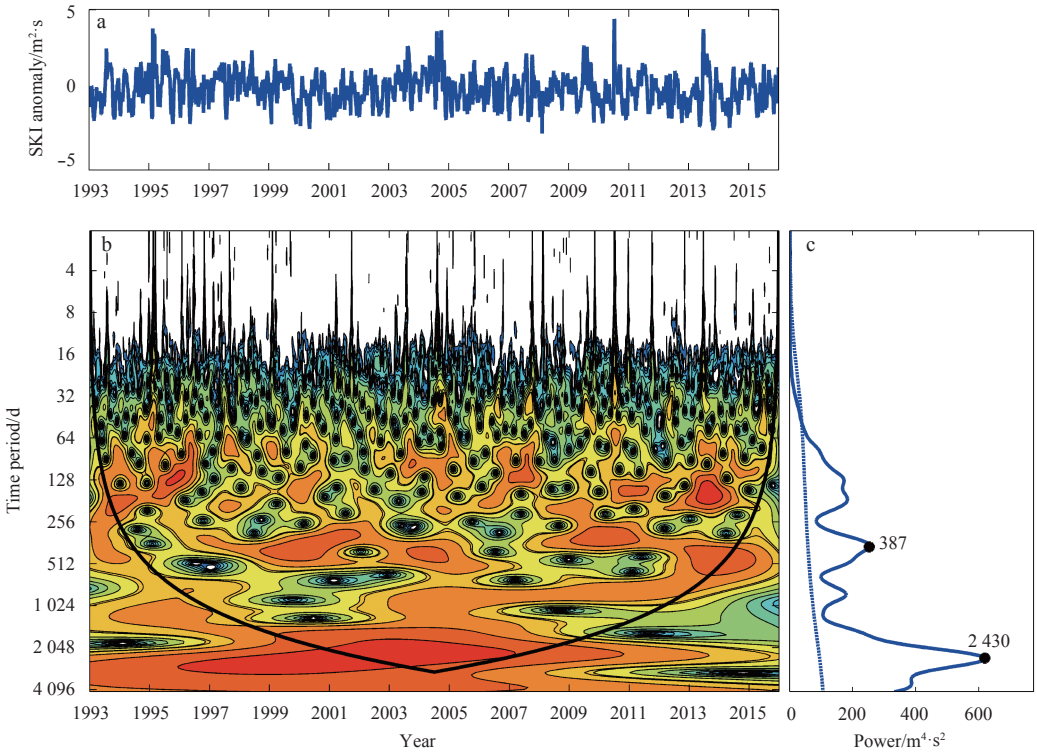

Fig. 2. Wavelet analysis of the surface Kuroshio intensity (SKI) time series at 23°N. a. The SKI anomaly time series, b. the local wavelet power spectra, and c. the averages of b over all times.

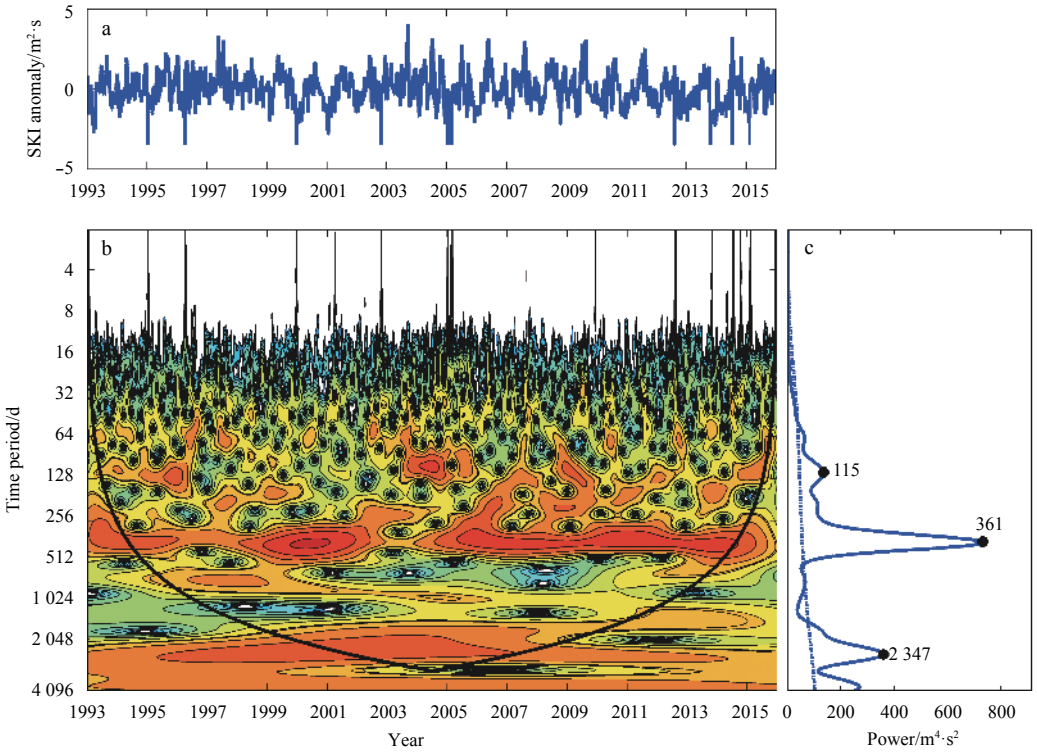

Fig. 3. Wavelet analysis of the surface Kuroshio intensity (SKI) time series at 25°N. a. The SKI anomaly time series, b. the local wavelet power spectra, and c. the averages of b over all times.

In addition, a significant test of the wavelet power spectrum of the eddy field was performed using the same method as described in Section 2.5. Finally, a comparison of wavelet power spectra between SKI and eddy field is shown in Fig. 5, where the blank areas are insignificant and the remaining areas passed the significance test.

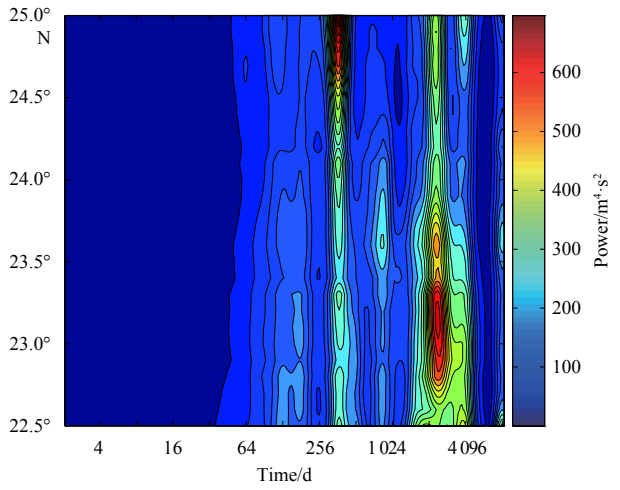

Fig. 4. The power spectrum of the time series for SKI at all latitudes from 22.5°N to 25°N. For example, the power spectrum data at 25°N is from Fig. 3c.

As shown in Fig. 5b, the eddy field east of Taiwan has four obvious periods: 200 days (0.55 year, semiannual period), 374 days (1 year, annual period), 889 days (2.43 years, first interannual period) and 2 374 days (6.5 years, second interannual period), generally corresponding to the four periods of the SKI (shown in Fig. 5a). There are also variations across latitudes in the same period. In addition, in the first period, the Kuroshio period ranged from 122 days to 192 days, and the eddy period ranged from 160 days to 240 days. The period of the two show an approximate correspondence.

4 Correlation analysis and cause analysis

4.1 *Correlation analysis*

In this study, we used the correlation analysis method described in Section 2.5 to calculate correlation coefficients between the time series of the SKI and the time series of eddy fields at different latitudes for the four different periods respectively. By using the time-lagged correlation analysis method, the correlation coefficients between the SKI and eddy fields for different lag time are calculated. A negative time lag (τ<0), indicates that the time of eddy field is earlier than that of the SKI, i.e., the eddy field leads the SKI. In contrast, a positive time lag (τ>0) indicates that the time of eddy field is later than that of the surface Kuroshio intensity, i.e., the time of eddy field $t+\tau$ corresponds to the SKI time t. Finally, a zero time lag indicates that the Kuroshio and eddy are in the same period. The correlation coefficient of the semiannual period between two series is shown in Fig. 8. Figure 9a shows this correlation coefficient after significance testing.

Figure 9 shows the correlation coefficient of all periods after significance testing. Blank areas are those that did not pass the significance test. It should be noted that the first interannual period of the Kuroshio in Fig. 7a did not pass the significance testing between 24.5°–25°N. In other words, the first interannual period is only obvious in the middle region, so only the results for 22.5°–24.5°N are shown in Fig. 9c. As shown, there are differences in the correlation coefficients at different latitudes. For example, the correlation coefficient in the semiannual and annual periods is relatively high at the 23.3°–25°N latitudes, indicating that the correlation between the Kuroshio and the eddy in this region is also high. The correlation coefficient of the first interannual period (~2.4 year-period) at the 22.7°–24.1°N latitudes is relatively large and negative, which indicates a high correlation between the Kuroshio and the eddy in this region, but with the opposite sign. The second interannual period (~6.5 year-period) has a high correlation at all latitudes (22.5°–25°N). Clearly, varying lag times have different correlation coefficients. For the semiannual period and first interannual period (2.4 year period), the

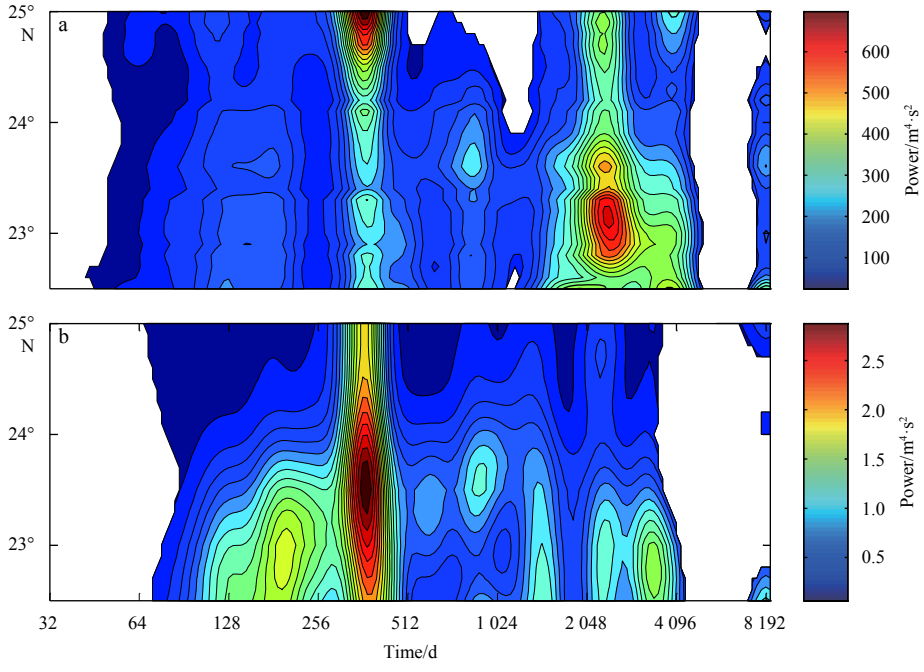

Fig. 5. The power spectrum comparison of the SKI (a) and surface eddy intensity (SEI) (b) time series at all latitudes from 22.5°N to 25°N after significance testing.

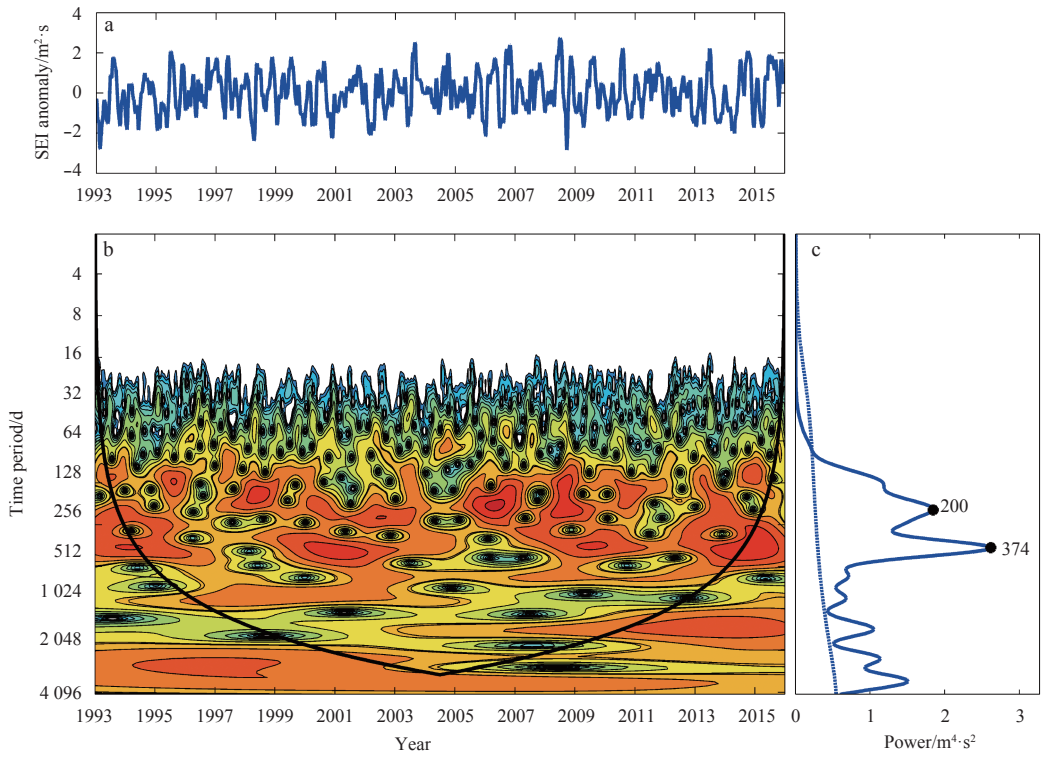

Fig. 6. Wavelet analysis of the SEI time series at 23°N. a. The eddy field time series (sea level anomaly), b. the local wavelet power spectra, and c. the averages of b for all times.

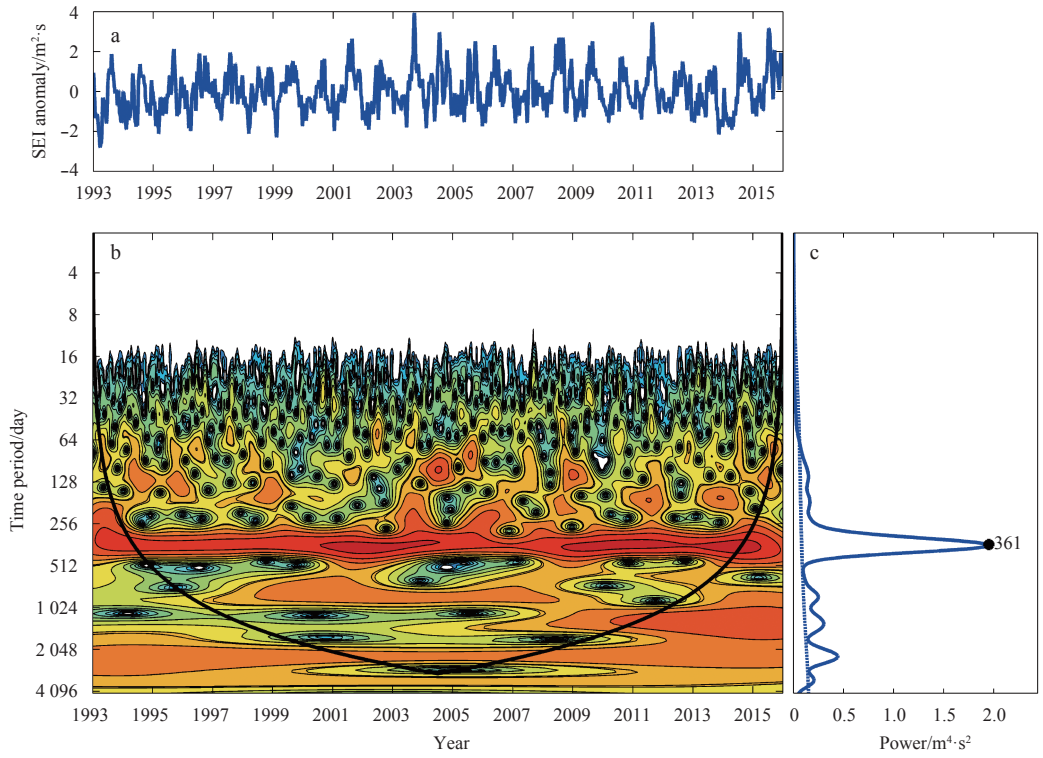

Fig. 7. Wavelet analysis of the SEI time series at 25°N. a. The eddy field time series (sea level anomaly), b. the local wavelet power spectra, and c. the averages of b for all times.

correlation seems to be systemic at the line where the lag time is zero. For the second interannual period, when the time lag is negative (τ<0), which means the time of eddy field time is earlier than that of the SKI, the correlation is mainly positive, whereas a positive time lag (τ>0) corresponds to a primarily negative correlation.

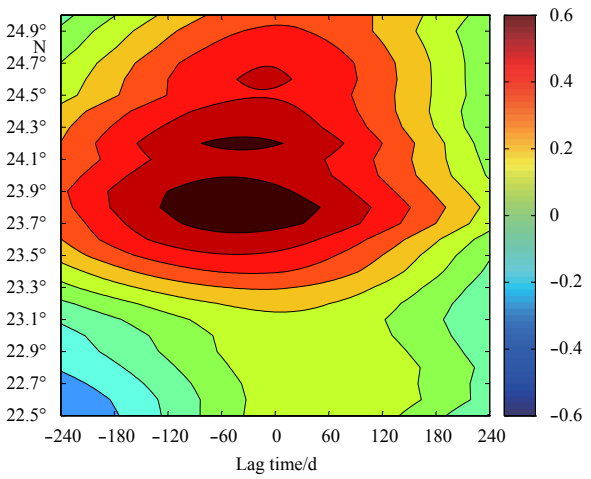

Fig. 8. Lagged correlation coefficient between the parts of SEI and SKI with a semiannual period.

4.2 *Causal analysis*

The causal analysis method described in Section 2.6 was applied to the SKI and eddies over the Kuroshio. We obtained the effects of the Kuroshio on the eddy field over the four periods and vice-versa. The lag time meaning is similar to the lag correlation analysis in Section 4.1. A schematic diagram of the first-period Kuroshio influence on eddies is provided as an example in Fig. 10.

To test the interaction between the two, we compare the absolute value of the effect of Kuroshio on the eddy in the four periods, i.e., τ_{12}. The impact of eddies on the Kuroshio, i.e., τ_{21}, was also compared. In the semiannual period, during the test of the impact of the Kuroshio on the eddy, $|\frac{\tau_{12}}{\tau_{21}}| \geqslant 1$ means that the data passed the test, while $|\frac{\tau_{12}}{\tau_{21}}| < 1$ indicates a failure to pass the test. For the impact of the eddy on the Kuroshio, $|\frac{\tau_{21}}{\tau_{12}}| \geqslant 1$ means that the data passes the test, while $|\frac{\tau_{21}}{\tau_{12}}| < 1$ indicates a failure to pass the test. Figure 11 shows effect of Kuroshio on eddy field and Figure 12 shows the influence of eddy field on the Kuroshio in all periods. The blank regions in Figs 11 and 12 indicate the failed tests.

As shown in Figs 11 and 12, the interaction between the Kuroshio and eddy field vary over periods and latitudes. For example, the influence of eddies on the Kuroshio is obvious in the semiannual period, primarily at the higher latitudes (23.9°–25°N) east of Taiwan. In the annual period, the Kuroshio has a greater impact on the eddy field at the high latitudes (23.9°–25°N). In the first interannual period (~2.4-year period), the eddy field has impact on the SKI. In the second interannual period (~6.5-year period), the eddy field has a larger impact on the SKI than SKI has on the eddy field.

5 Conclusions

Based on the satellite remote sensing data provided by AVISO center from January 1993 to December 2015, a total of 8 400 days, SKI and eddy field (sea level anomaly) data from adjacent waters (22.5°–25°N, 123°–124°E) in the east of Taiwan were analyzed using wavelet analysis. The results indicate there are four main periods of SKI and eddy field east of Taiwan. The correlation and causal relationship between the SKI and the nearby eddy field over the four corresponding periods have been studied. Our conclusions are as follows.

(1) Based on wavelet analysis, the SKI east of Taiwan shows significant seasonal, annual and interannual periods. In addition

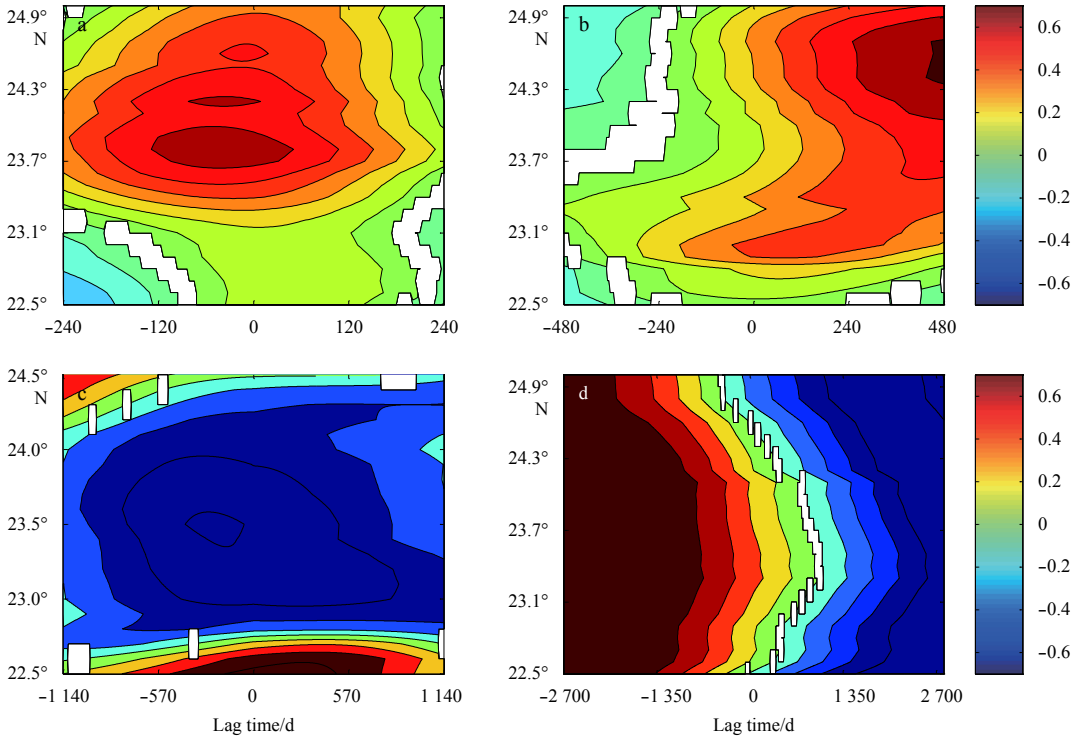

Fig. 9. Lagged correlation coefficient after significance testing between the SEI and SKI for different periods. a. The semiannual period, b. the annual period, c. the first interannual period, and d. the second interannual period.

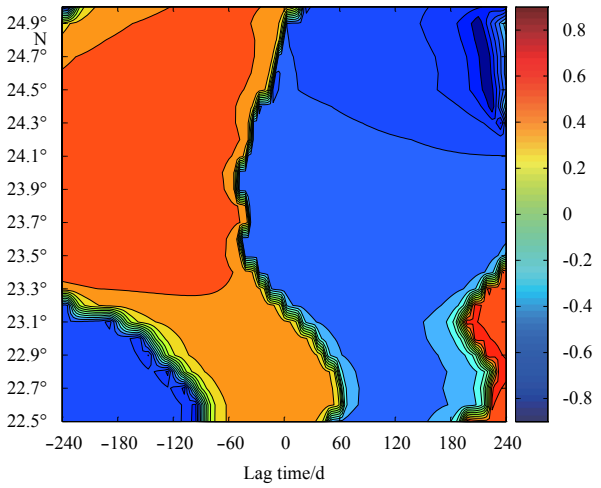

Fig. 10. Effect of surface Kuroshio intensity on the eddy field (τ_{12}) using the respective SEI and SKI with a semiannual period.

to the obvious periods of 182 days (0.5 year, the semiannual period) and 365 days (1 year, the annual period), there is also more obvious period about 860 days (2.35 years, the first interannual period) and 2 472 days (6.8 years, the second interannual period) for the SKI. Different latitudes correspond to different periods. The periodicity of the semiannual period and 2.35-year periods at the lower latitudes (22.5°–24°N) was more pronounced than that in the higher latitudes (24°–25°N) east of Taiwan. The annual and 6.8-year periods have obvious periodicity in all latitudes (22.5°–25°N), and the annual period has the most obvious periodicity at the high latitudes (24.5°–25°N). The period of the 6.8-year period is the most significant at the middle and low latitudes (22.7°–23.9°N).

(2) There are significant periods of eddy field east of the Kuroshio at 200 days (0.54 year, the semiannual period), 374 days (1 year, the annual period), 889 days (2.43 years, the first interannual period), and 2 374 days (6.5 years, the second interannual period), generally corresponding to the four periods of the SKI; similarly, there are differences at different latitudes in the same period. Four cycles have obvious periodicity for the whole latitudinal range of the study area (22.5°–25°N). Among them, the period of the semiannual period is the most obvious at the low latitudes (22.5°–23.5°N). The period of the annual period is most obvious in the middle and low latitudes (22.5°–24.5°N) and the 2.43-year period has more obvious periodicity at middle latitudes (23°–24°N). The 6.5-year period has obvious periodicity at the middle and low latitudes (22.5°–23.7°N).

(3) The correlations between the Kuroshio and eddy field are different at different latitudes of different periods. Correlations found in the semiannual period and annual period are more obvious at middle latitudes (23.3°–25°N). The correlation coefficient of the first interannual period (~2.4 year-period) at the latitudes 22.7°–24.1°N is relatively large and negative. The second interannual period (~6.5 year-period) had a high correlation in all latitudes (22.5°–25°N). Finally, with different lag times, the correlation coefficients are different.

(4) The causal relationship between the SKI and the eddy field varied with latitude and period. In the semiannual period, the influence of eddies on the Kuroshio is obvious, while in the annual period, the Kuroshio had a greater impact on the eddy field. In the first interannual period (~2.4-year period), the eddy field has impact on the surface Kuroshio intensity. In the second interannual period (~6.5-year period), the eddy field has a larger

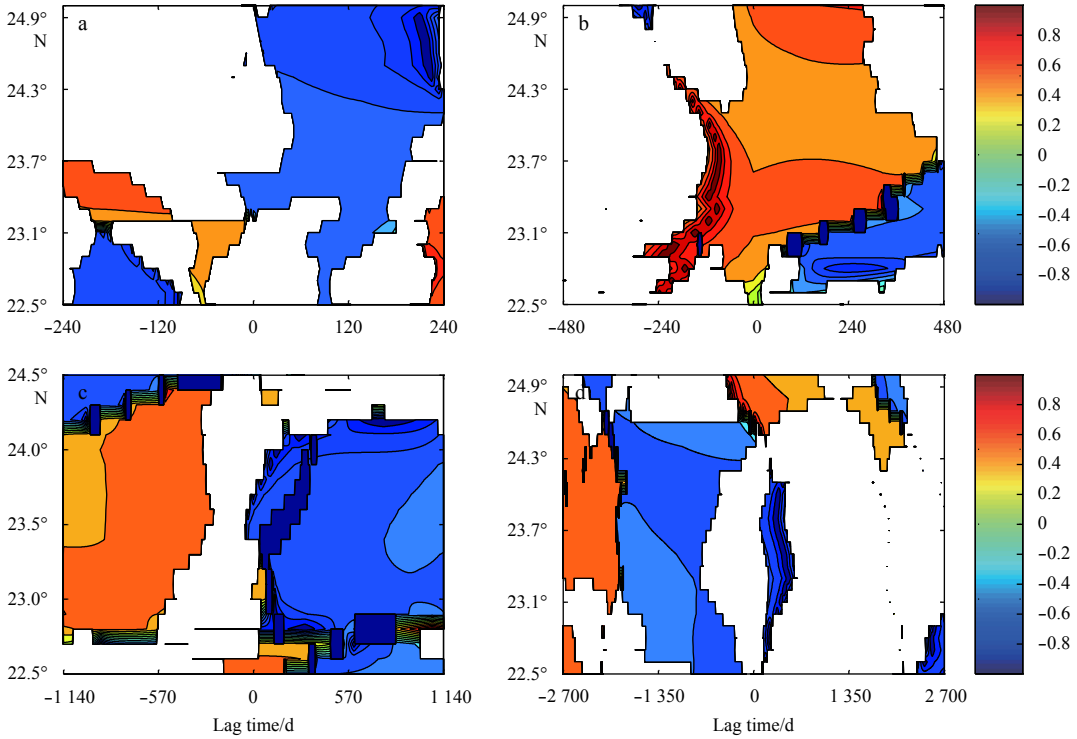

Fig. 11. Effect of the SKI on the SEI (τ_{12}) after significance testing over different periods. a. The semiannual period, b. the annual period, c. the first interannual period, and d. the second interannual period.

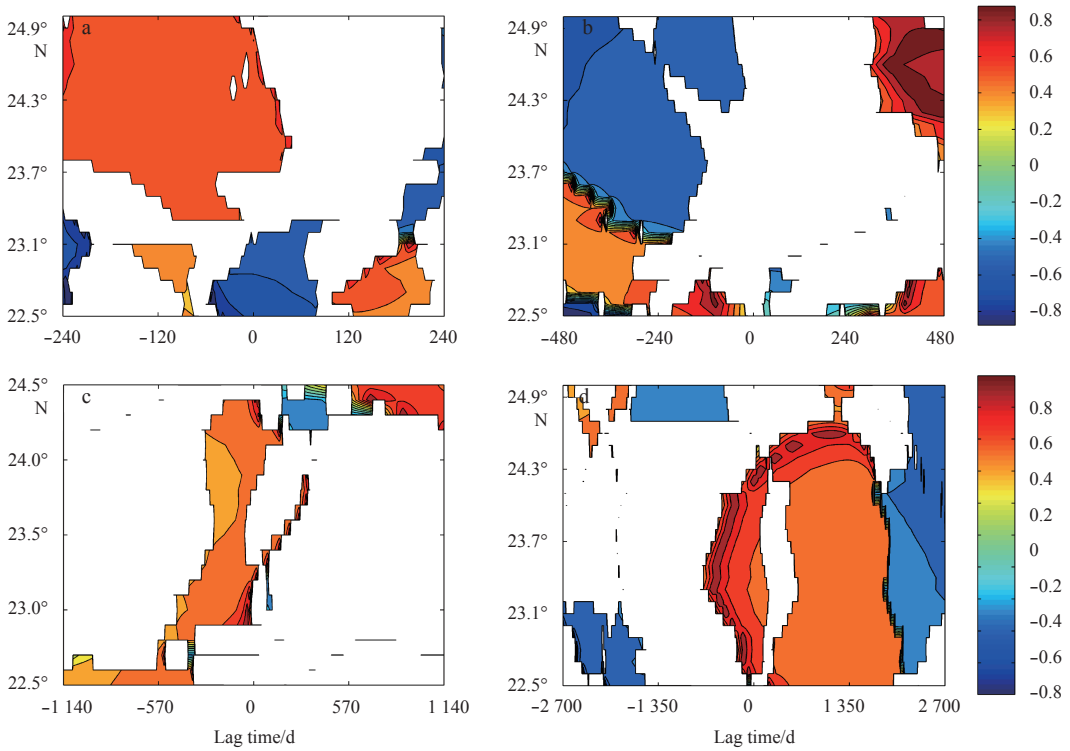

Fig. 12. Effect of the SEI on the SKI (τ_{21}) after significance testing over different periods. a. The semiannual period, b. the annual period, c. the first interannual period, and d. the second interannual period.

impact on the SKI than SKI has on the eddy field.

Acknowledgements

We thank Guihua Wang and Xiang San Liang for helpful conversations. The altimeter products used in this study were produced by Ssalto/Duacs and distributed by AVISO, with support from CNES (http://www.aviso.oceanobs.com/duacs/).

References

Ambe D, Imawaki S, Uchida H, et al. 2004. Estimating the kuroshio axis South of Japan using combination of satellite altimetry and drifting buoys. Journal of Oceanography, 60(2): 375–382, doi: 10.1023/B:JOCE.0000038343.31468.fe

Chang Yulin, Miyazawa Y, Guo Xinyu. 2015. Effects of the STCC eddies on the Kuroshio based on the 20-year JCOPE2 reanalysis results. Progress in Oceanography, 135: 64–76, doi: 10.1016/j.pocean.2015.04.006

Chang Y L, Oey L Y. 2011. Interannual and seasonal variations of Kuroshio transport east of Taiwan inferred from 29 years of tide - gauge data. Geophysical Research Letters, 38(8): L08603

Chelton D B, Schlax M G, Samelson R M. 2011. Global observations of nonlinear mesoscale eddies. Progress in Oceanography, 91(2): 167–216, doi: 10.1016/j.pocean.2011.01.002

Cheng Y H, Ho C R, Zheng Quanan, et al. 2017. Statistical features of eddies approaching the Kuroshio east of Taiwan Island and Luzon Island. Journal of Oceanography, 73(4): 427–438, doi: 10.1007/s10872-017-0411-7

Delman A S, Mcclean J L, Sprintall J, et al. 2015. Effects of eddy vorticity forcing on the mean state of the Kuroshio extension. Journal of Physical Oceanography, 45(5): 1356–1375, doi: 10.1175/JPO-D-13-0259.1

Gawarkiewicz G, Jan S, Lermusiaux P F J, et al. 2011. Circulation and intrusions northeast of Taiwan: Chasing and predicting uncertainty in the cold dome. Oceanography, 24(4): 110–121, doi: 10.5670/oceanog

Geng Wu, Xie Qiang, Chen Gengxin, et al. 2016. Numerical study on the eddy–mean flow interaction between a cyclonic eddy and Kuroshio. Journal of Oceanography, 72(5): 727–745, doi: 10.1007/s10872-016-0366-0

Geng Wu, Xie Qiang, Chen Gengxin, et al. 2018. A three-dimensional modeling study on eddy-mean flow interaction between a Gaussian-type anticyclonic eddy and Kuroshio. Journal of Oceanography, 74(1): 23–37, doi: 10.1007/s10872-017-0435-z

Hsin Y C, Chiang T L, Wu C R. 2011. Fluctuations of the thermal fronts off northeastern Taiwan. Journal of Geophysical Research: Oceans, 116(C10): C10005, doi: 10.1029/2011JC007066

Hsin Y C, Qiu Bo, Chiang T L, et al. 2013. Seasonal to interannual variations in the intensity and central position of the surface Kuroshio east of Taiwan. Journal of Geophysical Research: Oceans, 118(9): 4305–4316, doi: 10.1002/jgrc.20323

Hsu P C, Lin C C, Huang S J, et al. 2016. Effects of cold eddy on Kuroshio Meander and its surface properties, east of Taiwan. IEEE Journal of Selected Topics in Applied Earth Observations and Remote Sensing, 9(11): 5055–5063, doi: 10.1109/JSTARS.2016.2524698

Hwang C, Wu C R, Kao R. 2004. TOPEX/Poseidon observations of mesoscale eddies over the Subtropical countercurrent: kinematic characteristics of an anticyclonic eddy and a cyclonic eddy. Journal of Geophysical Research: Oceans, 109(C8): C08013

Ichikawa K, Tokeshi R, Kashima M, et al. 2008. Kuroshio variations in the upstream region as seen by HF radar and satellite altimetry data. International Journal of Remote Sensing, 29(21): 6417–6426, doi: 10.1080/01431160802175454

Jan S, Yang Y J, Wang J, et al. 2015. Large variability of the Kuroshio at 23.75°N east of Taiwan. Journal of Geophysical Research: Oceans, 120(3): 1825–1840, doi: 10.1002/2014JC010614

Johns W E, Lee T N, Zhang Dongxiao, et al. 2001. The kuroshio east of Taiwan: moored transport observations from the WOCE PCM-1 array. Journal of Physical Oceanography, 31(4): 1031–1053, doi: 10.1175/1520-0485(2001)031<1031:TKEOTM>2.0.CO;2

Kuo Y C, Chern C S, Zheng Zhewen. 2017. Numerical study on the interactions between the Kuroshio current in the Luzon Strait

and a mesoscale eddy. Ocean Dynamics, 67(3–4): 369–381
Lee I H, Dong S K, Wang Yuhuai, et al. 2013. The mesoscale eddies and Kuroshio transport in the western North Pacific east of Taiwan from 8-year (2003–2010) model reanalysis. Ocean Dynamics, 63(9-10): 1027–1040, doi: 10.1007/s10236-013-0643-z
Liang X S. 2014. Unraveling the cause-effect relation between time series. Physical Review E, 90(5): 052150, doi: 10.1103/PhysRevE.90.052150
Liang X S. 2015. Normalizing the causality between time series. Physical Review E, 92(2): 022126
Lien R C, Ma B, Cheng Y H, et al. 2014. Modulation of Kuroshio transport by mesoscale eddies at the Luzon Strait entrance. Journal of Geophysical Research: Oceans, 119(4): 2129–2142, doi: 10.1002/2013JC009548
Liu Yu, Dong Changming, Liu Xiaohui, et al. 2017. Antisymmetry of oceanic eddies across the Kuroshio over a shelfbreak. Scientific Reports, 7: 6761, doi: 10.1038/s41598-017-07059-1
Ma Libin, Wang Qiang. 2014. Interannual variations in energy conversion and interaction between the mesoscale eddy field and mean flow in the Kuroshio south of Japan. Chinese Journal of Oceanology and Limnology, 32(1): 210–222, doi: 10.1007/s00343-014-3036-3
Ma Xiaohui, Jing Zhao, Chang Ping, et al. 2016. Western boundary currents regulated by interaction between ocean eddies and the atmosphere. Nature, 535(7613): 533–537, doi: 10.1038/nature18640
Miyazawa Y, Guo Xinyu, Yamagata T. 2004. Roles of mesoscale eddies in the Kuroshio paths. Journal of Physical Oceanography, 34(10): 2203–2222, doi: 10.1175/1520-0485(2004)034<2203:ROMEIT>2.0.CO;2
Nan Feng, Xue Huijie, Chai Fei, et al. 2011b. Identification of different types of Kuroshio intrusion into the South China Sea. Ocean Dynamics, 61(9): 1291–1304, doi: 10.1007/s10236-011-0426-3
Nan Feng, Xue Huijie, Xiu Peng, et al. 2011a. Oceanic eddy formation and propagation southwest of Taiwan. Journal of Geophysical Research: Oceans, 116(C12): C12045, doi: 10.1029/2011JC007386
Qiu Bo, Chen Shuming. 2010a. Interannual variability of the North Pacific subtropical countercurrent and its associated mesoscale eddy field. Journal of Physical Oceanography, 40(1): 213–225, doi: 10.1175/2009JPO4285.1
Qiu Bo, Chen Shuming. 2010b. Eddy-mean flow interaction in the decadally modulating Kuroshio Extension system. Deep Sea Research Part II: Topical Studies in Oceanography, 57(13–14): 1098–1110
Torrence C, Compo G P. 1998. A practical guide to wavelet analysis. Bulletin of the American Meteorological Society, 79(1): 61–78, doi: 10.1175/1520-0477(1998)079<0061:APGTWA>2.0.CO;2
Tsai C, Andres M, Jan S, et al. 2015. Eddy-Kuroshio interaction processes revealed by mooring observations off Taiwan and Luzon. Geophysical Research Letters, 42(19): 8098–8105, doi: 10.1002/2015GL065814
Wang Guihua, Su Jilan, Chu P C. 2003. Mesoscale eddies in the South China Sea observed with altimeter data. Geophysical Research Letters, 30(21): 2121, doi: 10.1029/2003GL018532
Wang Huizan, Wei Linjin, Zhang Quanli, et al. 2018. Identification of the Kuroshio Path East of Taiwan and its Variation. Oceanologia et Limnologia Sinica , 49(2): 271–279
Waseda T, Mitsudera H, Taguchi B, et al. 2002. On the eddy-Kuroshio interaction: Evolution of the mesoscale eddy. Journal of Geophysical Research: Oceans, 107(C8): 3088, doi: 10.1029/2000JC000756
Yan Xiaomei, Zhu Xiaohua, Pang Chongguang, et al. 2016. Effects of mesoscale eddies on the volume transport and branch pattern of the Kuroshio east of Taiwan. Journal of Geophysical Research: Oceans, 121(10): 7683–7700, doi: 10.1002/2016JC012038
Yang Y, Liu C T, Hu J H, et al. 1999. Taiwan current (Kuroshio) and impinging eddies. Journal of Oceanography, 55(5): 609–617, doi: 10.1023/A:1007892819134
Yang Xiaodan, Mao Xinyan, Jiang Wensheng. 2014. Study of the sea surface height key region which reveals the variability of the Kuroshio volume transport east of Taiwan. Transactions of Oceanology and Limnology (in Chinese), 37(1): 1–6
Yin Yuqi, Lin Xiaopei, He Ruoying, et al. 2017. Impact of mesoscale eddies on Kuroshio intrusion variability northeast of Taiwan. Journal of Geophysical Research: Oceans, 122(4): 3021–3040, doi: 10.1002/2016JC012263
Yu Dandan, Zhang Ren, Hong Mei, et al. 2007. Correlation analysis between the west pacific subtropical high and the East Asian summer monsoon system based on cross wavelet and wavelet coherence. Journal of Nanjing Institute of Meteorology (in Chinese), 30(6): 755–769
Zhang Dongxiao, Lee T N, Johns W E, et al. 2001. The Kuroshio east of Taiwan: Modes of variability and relationship to interior ocean mesoscale eddies. Journal of Physical Oceanography, 31(4): 1054–1074, doi: 10.1175/1520-0485(2001)031<1054:TKEOTM>2.0.CO;2
Zhang Zhiwei, Zhao Wei, Qiu Bo, et al. 2017. Anticyclonic Eddy Sheddings from Kuroshio loop and the accompanying cyclonic eddy in the northeastern South China Sea. Journal of Physical Oceanography, 47(6): 1243–1259, doi: 10.1175/JPO-D-16-0185.1
Zheng Quanan, Tai C K, Hu Jiangyu, et al. 2011. Satellite altimeter observations of nonlinear Rossby eddy–Kuroshio interaction at the Luzon Strait. Journal of Oceanography, 67: 365–376, doi: 10.1007/s10872-011-0035-2
Zheng Quanan, Xie Lingling, Zheng Zhiwen, et al. 2017. Progress in research of mesoscale eddies in the South China Sea. Advances in Marine Science (in Chinese), 35(2): 131–158